doi:10.11835/j.issn.1671-8224.2018.01.01

To cite this article: SUN Jie, ZHANG Zi-xin, HUANG Xin, JU Xin. Construction of an ultra-deep diaphragm wall: a case study [J]. J Chongqing Univ Eng Ed [ISSN 1671-8224], 2018, 17(1): 1-16.

Construction of an ultra-deep diaphragm wall: a case study *

SUN Jie †, ZHANG Zi-xin, HUANG Xin ‡, JU Xin

Department of Geotechnical Engineering, Tongji University, Shanghai 200092, P. R. China

Key Laboratory of Geotechnical and Underground Engineering of the Ministry of Education, Tongji University, Shanghai 200092, P. R. China

Received 11 May 2017; received in revised form 11 July 2017

Abstract: This paper presents a case study on an ultra-deep diaphragm wall with a depth of 110 m constructed in Ningbo City. The in-situ application shows that using Bauer BC40 cutter machine in conjunction with cutter wheels specified for different strata would be qualified for constructing the 110 m diaphragm wall with high efficiency and precision given that the quality of slurry and poured concrete can be guaranteed. The ground settlement can be effectively controlled by using the overlapping construction method. Sliding failure as a whole characterized by pronounced lateral deformation is likely to occur in the upper muddy clay layer due to its high compressibility and sensitivity. In contrast, local collapse of trench walls tends to happen in the sandy silt strata. Furthermore, careful attention should be paid to sandy silt during the entire construction period as the vertical displacement of the sandy silt continues to develop even after concrete pouring.

Keywords: diaphragm wall; soft soil; quality control; settlement; overlapping method; trench cutter BC40

CLC number: TU92 Document code: A

1 Introduction

Nowadays, waterlogging and underground sewage overflow have become an increasingly serious issue afflicting the life of citizens in big cities during rainy seasons [1-2]. The origins of this problem come from two aspects: 1) a large number of green fields and reservoirs have been reclaimed to spare space for constructing high-rise buildings or estates during the rapid urbanization process, which greatly reduces the city's natural capacity to resist flooding and water-logging; 2) most drainage systems in old urban districts are out-of-date and with low drainage standards. Therefore, upgrading the storage and drainage system has become an urgent task. Considering the congested surface facilities and saturated shallow underground space, construction of deeply-buried water storage and drainage tunnels which are normally located about 50 m to 100 m beneath the ground surface has become

† SUN Jie (孙杰): 542420281@qq.com.

‡ Corresponding author, HUANG Xin (黄昕):xhuang@tongji.edu.cn.

* Funded by the National Basic Research Program of China (973 Program, No.2014CB046905), the National Natural Science Foundation of China (Grant Nos. 41172249 and 51509186), and the State Key Laboratory for Geomechanics and Deep Underground Engineering (No. SKLGDUEK1303), and the funding provided by Zhuhai Da Heng Qin Company Limited (Grant No. SG25-2014-173B1).

a laudable solution [3-4]. Firstly, it leaves the shallow underground space to subways and other municipal facilities; secondly, construction of a deeply-buried tunnel usually adopts shield tunneling method, which causes relatively small disturbances to surrounding ground; thirdly, the deeply-buried water storage and drainage tunnel can also complement the old shallow drainage system to form comprehensive drainage networks, which is an economical way to greatly improve the capacity of flood control and drainage. To date, there has been such practices in several countries including the United States, the United Kingdom, Japan, Singapore, and Mexico.

China is now boosting the 'sponge city' program to upgrade the drainage system of modern cities. As one of the earliest batch of cities to implement the 'sponge city' program, Shanghai has outlined a comprehensive and powerful water storage and drainage system. In particular, as the precursor of the new water storage and drainage system, the Suzhou River deeply-buried tunnel project was scheduled to start in 2017. The main tunnel was designed to be 15 km in length with eight ultra-deep shafts being arranged along both sides of the Suzhou River. The average depth of designed diaphragm walls reaches 110 m, which once completed will become the deepest diaphragm wall project in soft soil areas of China.

A primary issue needed to be solved for the Suzhou River deeply-buried tunnel project is the construction of the ultra-deep shafts which serve as the launching and receiving pits of the shield tunneling machines. The two prevailing technologies to construct an ultra-deep shaft in soft grounds are the caisson method and the diaphragm wall method [5]. Practicing experience reveals that the vertical accuracy of the caisson method is lower than the diaphragm wall method. Furthermore, the construction efficiency of caisson can be greatly reduced with the increase of sinking depth. Therefore, the diaphragm wall method is more frequently adopted when constructing the deeply-buried tunnel. A typical example is the famous Tokyo underground storm-water storage tunnel project completed in 2006 with a storage capacity of approximately 120 000 m^3 [6]. The diaphragm wall of the No. 3 shaft of this project has an excavation depth of 144 m, which is currently the deepest diaphragm wall in Japan.

As shown by Cowland et al. [7], the ground settlement caused by the construction of diaphragm wall may account for 30% to 50% of the total settlement induced by 'cut-and-cover' excavations. Therefore, mitigating the disturbance of diaphragm wall construction to the surrounding ground is of great importance. Considering the soft nature and layered formation of soils along the diaphragm wall depth of the Suzhou River deeply-buried tunnel project [8], it can be foreseen that high requirements will be imposed on trenching equipment capacity, precision control, slot stability, quality control, water tightness of joints as well as construction efficiency. Furthermore, despite a variety of studies on the construction of diaphragm walls including full-scale tests [9-13], laboratory experiments [14-16], and analytical and numerical analyses [17-19], case studies on construction of ultra-deep diaphragm wall are rarely reported. Since this is the first time to construct such a deep diaphragm wall in soft soil areas of China, it is necessary to carry out an in-situ test before the start of the real project.

Considering that Ningbo has ground conditions similar to Shanghai, some parts of a 77 m deep diaphragm wall in Ningbo were extended to 110 m. In-situ tests were carried out aiming at assessing the feasibility of constructing an ultra-deep diaphragm wall with a depth greater than 100 m in soft soil areas, such as Ningbo and Shanghai. The effectiveness and applicability of selected trenching technology and quality control measures were evaluated and the ground responses were monitored.

2 Overview of the 110 m diaphragm wall project

A plan view of the trial diaphragm wall site is shown in Fig. 1. It was a part of the propping structure for the excavation of Children's Park Station which was a transition station of Metro Line 3 and Line 4 in Ningbo City, Zhejiang Province of China. The original design depth of the diaphragm wall was 77 m. The three adjacent panels were extended to 110 m and served as the testing panels for the deeply-buried tunnel project. Two of these three panels were primary panels (A2-a57, A2-a58), and the one in between was a secondary panel (A2-b59). The three panels had the same thickness of 1.0 m and the same depth of 110 m but differed in width with the width of the primary panels being 4.6 m and that of the secondary panel being 2.8 m.

A geotechnical investigation was carried out to identify the characteristics of ground conditions at the testing site. Fig. 2 shows the soil profile and soil properties along the depth of the testing diaphragm wall. The properties included the coefficient of compressibility $a_{0.1\sim0.2}$ and cone resistance $\mathrm{CPT}-q_u$. The underground water table was at about 2.5 m below the ground surface. The ground could be generally divided into three main regions: (a) the clayey region (0 to −31.2 m) in which the muddy clay layer was in a plastic flow state with high compressibility and a sensitivity as high as 4.4; (b) the sandy region (−31.2 m to −97.8 m) in which the medium dense sandy silt layer (−31.2 m to −48.0 m) had a non-uniformed gradation, and 80% of which were fine particles with diameters smaller than 0.05 mm; and (c) the underlying bedrock region below the depth of −97.8 m which was classified as medially to strongly-weathered shaly sandstone with a RQD (rock quality designation) of 50% to 80%. The toe of the diaphragm wall resided in this shaly sandstone layer. The physical and mechanical properties of each soil layer are listed in Table 1.

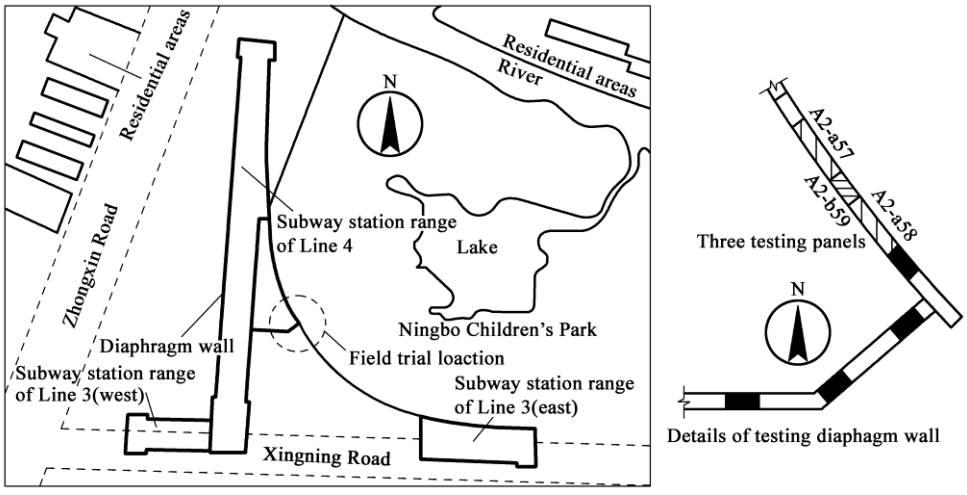

Fig. 1 Plan view of the trial project site

Table 1 Properties of soil strata at the testing site

Serial No.	Layer	Thickness /m	γ /(kN m^{-3})	ω/%	c/kPa	φ/(°)	v
1	Muddy clay	10.9	17.6	44.1	10.0	12.0	0.35
2	Silty clay	18.3	18.8	30.9	15.0	18.0	0.35
3	Sandy silt	16.8	18.6	26.1	1.7	25.4	0.30
4	Fine sand	27.2	19.0	29.1	0.0	19.0	0.25
5	Silty clay	9.1	18.9	32.1	28.0	28.0	0.30
6	Fine sand	13.5	19.0	29.6	0.0	19.0	0.25
7	Shaly sandstone	>20.0	2.1				

Notes: γ is the unit weight of soil; ω is the water content; c is the cohesion; φ is the internal friction angle; and v is the Poisson ratio.

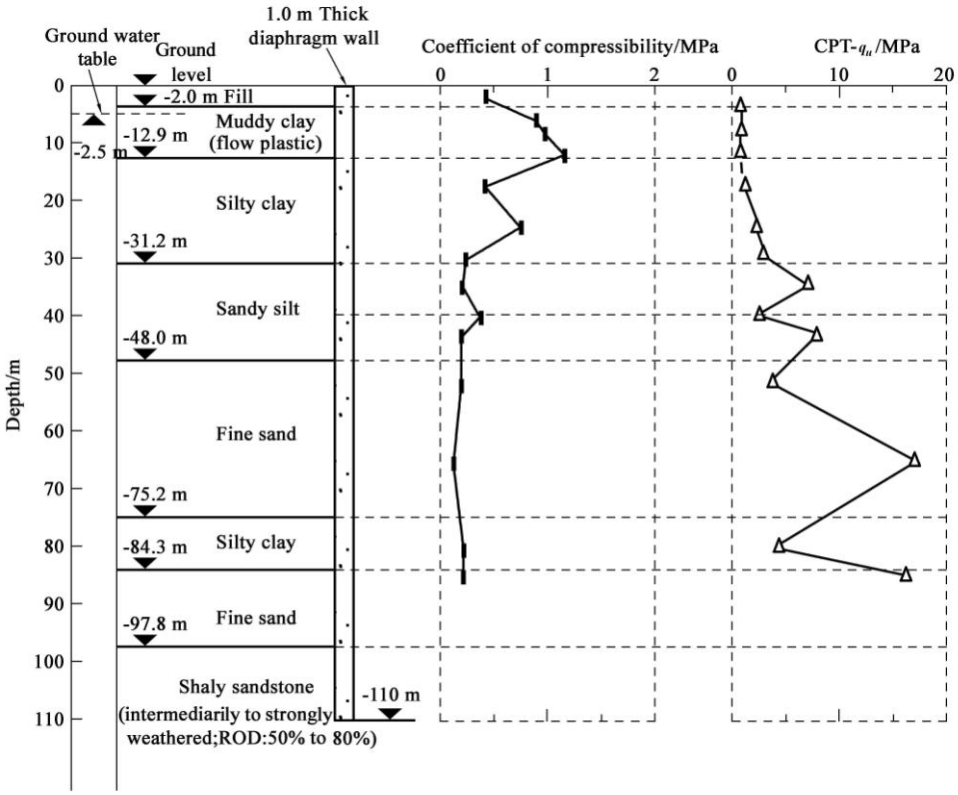

Fig. 2 Ground profile at the testing site

3 Key construction technologies and quality control measures

3.1 Overlapping method

Generally, construction difficulty of joints between individual panels increases as the wall depth increases [20]. Due to the low stiffness and low shearing and bending resistances, the waterproof performance of joints constructed by using the traditional top-end-tube method is relatively poor. Therefore, the applicability of the top-end-tube method is limited to diaphragm walls with a relatively shallow depth. In the current project, the overlapping method which utilizes the shear strength of the concrete was employed to construct panel joints [21].

The principle of overlapping method is illustrated in Fig. 3. The excavation sequence of the overlapping method is the same as the top-end-tube method, i.e., constructing the two primary panels first followed by the excavation of the secondary panel in between. However, when excavating the secondary panel, not only the soils within the secondary panel region but also part of the casted concrete of the two adjacent primary panels are cut by the cutter wheels. This results in a serrated but clean contact surface on the primary panels, which helps to form tight joints between the old concrete of primary panels and the newly-poured concrete of the secondary panel. The overlapping technique produces high-quality joints which are capable of transmitting shear forces and are sufficiently watertight without using artificial construction joint elements. The overlapping width between the cutter and the primary panel depends on the trench depth. Fig. 4 shows the dimensions and excavation sequence of the three testing panels. Considering the initial positioning error of cutter machine and the vertical deviation accumulated along the trenching depth, the overlapping width was set to be 30 cm to ensure that the minimum overlapping thickness is larger than 5 cm.

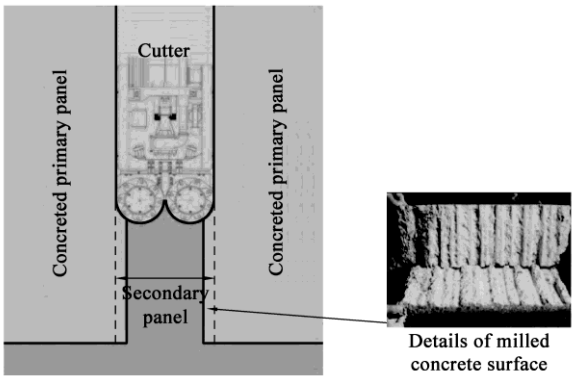

Fig. 3 The principle of overlapping method

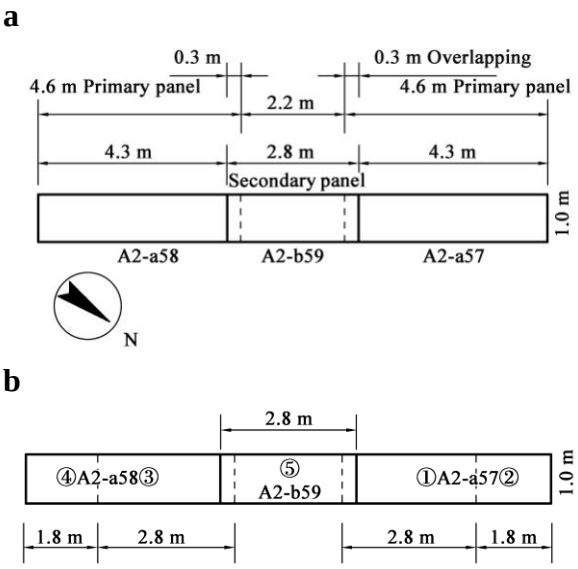

Fig. 4 The dimensions and excavation sequence of the three testing panels: a) Dimensions of three panels; b) excavation sequence of three testing panels

3.2 Cutter technology

Bauer trench cutter BC40, as shown in Fig. 5, was used in the current project; and its key operation parameters are listed in Table 2. One of the problems brought about by the great excavation depth is that the trench cutter will encounter multiple strata which are of large differences in both physical and mechanical

properties. Therefore, selecting the types of cutter wheels specified for different strata is essential.

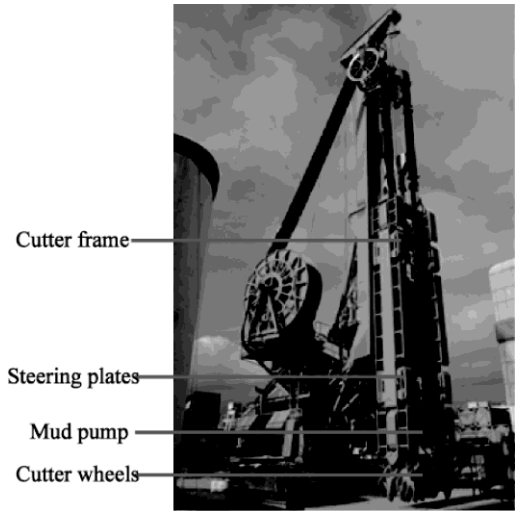

Fig. 5 Bauer BC40 trench cutter system / trench cutter principle sketch

Table 2 Key operation parameters of the Bauer trench cutter BC40

Gearbox	2×BCF10
Torque max.	100 kN m
Speed of rotation	0 to 25 r/min
Cutter length	2 500 mm to 3 200 mm
Cutter width	800 mm to 1 800 mm
Overall height	12.6 m
Maximum delivery rate, mud pump	450 m^3/h
Mass	41 t

Fig. 6 shows the three types of cutter wheels of Bauer BC40: (a) standard cutter wheels which are equipped with a large number of differently shaped tungsten carbide-tipped teeth and are primarily used in mixed soils; (b) round shank-chisel cutter wheels which are equipped with special round shank chisels and are primarily designed for cutting cemented sands, conglomerates, cobbles and weathered rock; (c) roller bit cutter wheel which is generated by fixing additional ballast to the cutter frame and is designed for extremely hard rock mass. The standard cutter wheels were employed to perform excavation in the uppermost clay, sand and strongly-weathered mudstone. Then the standard cutter wheels were replaced by the round shank chisel-cutter wheels when the cutter drilled into the medially weathered mudstone with a higher strength. The roller bit-cutter wheel was not used in this test project. This tactic helped to reduce the risk of the cutter wheel being wrapped up by muds and soil grains, which at the meantime guaranteed the construction efficiency.

Additional construction measures were also taken to mitigate the risk of cutter wheel being wrapped up by mud and soil grains during the real construction process: (a) reducing the dropping velocity of cutter wheel, so that the H/V (where H denotes the torque delivered by the cutter wheels, V denotes the crowd force characterized by the cutter's self-weight) can be optimized, as schematically shown in Fig. 7; (b) hoisting the milling wheel and getting rid of the soil adhering to the cutter wheel via forward and backward rotations; and (c) in case neither measures work, the wrapped-up muds and soil grains on the wheel will be cleaned up manually.

The verticality of the trench cutter was monitored by inclinometers integrated into the cutter system as illustrated in Fig. 8a. The cutter positions were adjusted by hydraulically-operated steering plates to ensure the verticality of the cutter. Additionally, a positioning frame was fixed on the guide wall of the trench as shown in Fig. 8b, which was used to mitigate the vibration of the cutter wheel during the initial milling process.

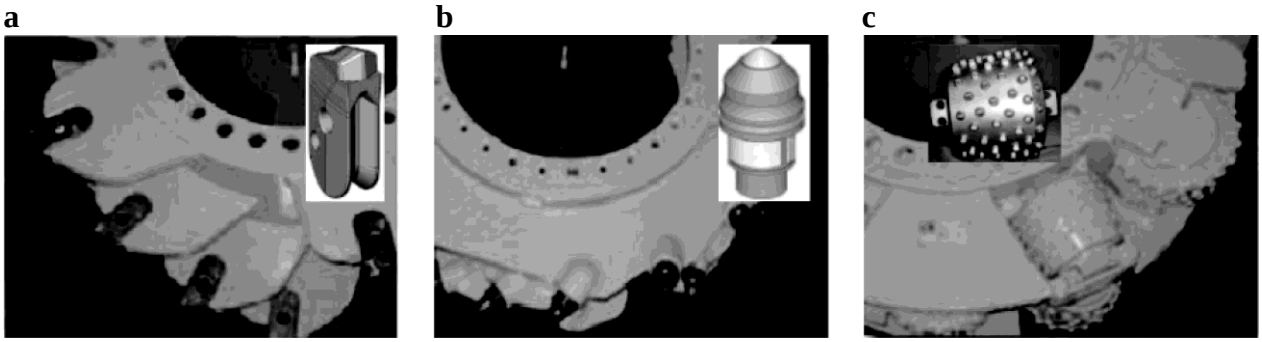

Fig. 6 Different types of cutter teeth: a) standard cutter wheel; b) round shank chisel-cutter wheel; and c) roller bit-cutter wheel [22]

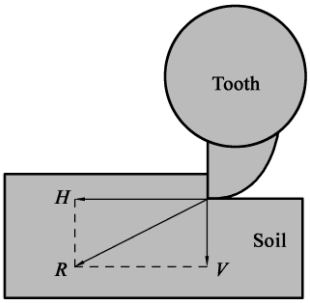

Fig. 7 *H*/*V* ratio of the cutter teeth of a trench cutter [23]

Ultrasonic testing was conducted to the three panels respectively upon the completion of trenching. The ultrasonic sounding profiles of each trench faces are shown in Fig. 9. It can be seen that the quality of the secondary panel (A2-b59) was poorer than the primary panels with the maximum verticality deviation located mainly at the upper portion of the trench reaching around 11 cm. Overall, the absolute deviation from the vertical direction for all three panels was controlled within the range of 0.10% with respect to the excavation depth, indicating that the accuracy of excavation satisfied the design requirement.

Fig. 10 shows the relationships between the excavation time and excavation depth for the three testing panels. The time to excavate the secondary panel (A2-b59) almost doubled that spent to excavate the primary panels (A2-a57 and A2-a58). In addition, the excavation rate decreased greatly when the cutter wheel entered the shaly sandstone stratum, i.e., the time spent to excavate the 12 m thick rock stratum was about 50% of the total excavation time of the 110 m diaphragm wall. Even so, the overall excavation rate of this testing section was practically acceptable.

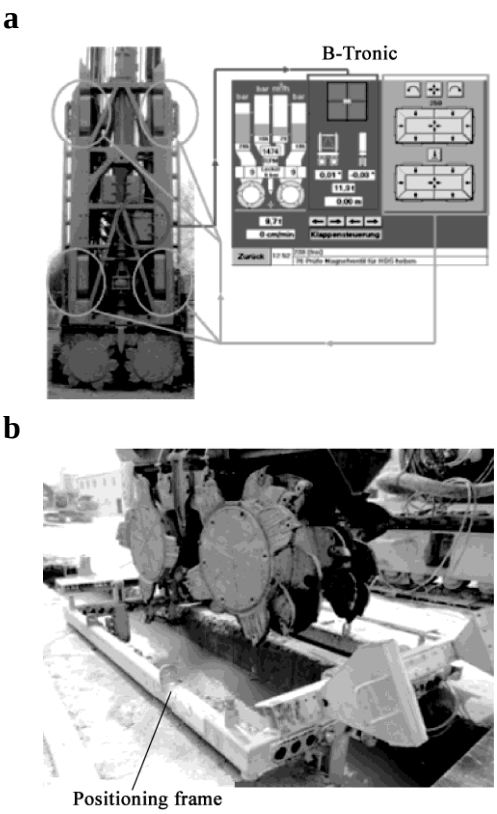

Fig. 8 The precision control of trenching: a) inclinometer system [20]; b) positioning frame

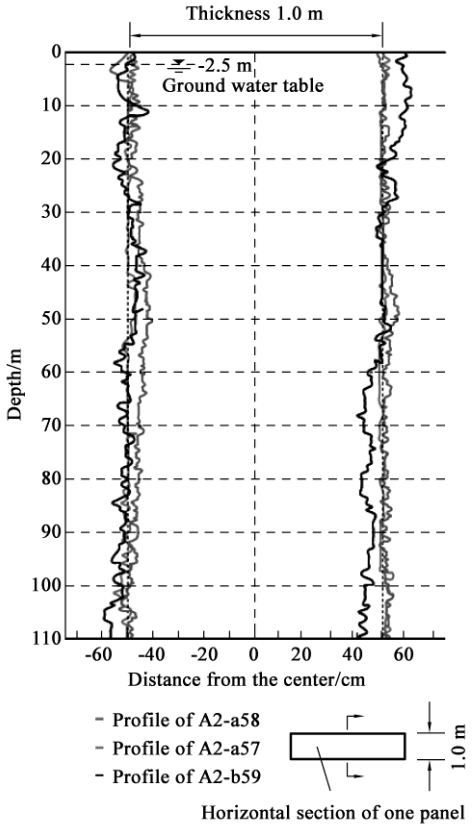

Fig. 9 Ultrasonic sounding profiles of trench faces

3.3 Quality control of the slurry

The quality control of slurry is crucial to maintain the stability of the trench wall and poured concrete. Another purpose of quality control of the slurry is to make it recyclable, and thereby reduce the cost of mud disposal [24-25]. However, as trench cutting processes, soil particles will be mixed up with the slurry, which thereby increases the unit weight and deteriorates the quality of the slurry. The deterioration rate of slurry could be greatly accelerated under the following circumstances: a) when trenching in sandy and silt layers, and b) during the cut of the secondary panel when the slurry is mixed up with massive Ca^{2+} inherited from concrete overcutting. To maintain the slurry quality, strict management measures must be carried out. The key to maintain the slurry quality is to timely separate the sandy and rocky particles from the contaminated slurry. This is achieved by employing the Bauer BE-500 desanding system which removes the soil particles in three stages in a descending order of particle size (>0.06 mm, between 0.04 mm and 0.06 mm, and between 0.026mm and 0.04mm) through the vibrating screen and cyclone. The largest processing capacity of the system can be up to 400 m^3/h. The key indexes of slurry are tested during the trenching process. Table 3 gives the mean values of those indexes at different stages. The magnitudes of the indexes, including proportion of mud, viscosity, sand content and PH, are all within the practically reasonable ranges, which shows that the adopted mud separation system can satisfy the requirements of constructing the 110 m deep diaphragm wall.

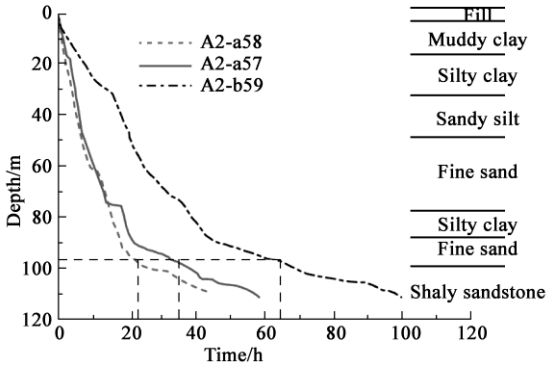

Fig. 10 Variation of excavation time of three panels with depth

Table 3 The monitored indexes of slurry during the whole trenching process

Description	Specific gravity	Viscosity/s	Mass fraction of Sand /%	PH
Fresh	1.035	28		9
Working	1.320	35	>10	11
Concreting	1.050	30	3	9
Required	<1.150	20 to 30	<7	8 to 10

Notes: The specific gravity was tested by a mud hydrometer; the viscosity by a 700 mL funnel; the mass fraction of sand by a sand ratio meter; and PH by PH test paper.

3.4 Quality control of concrete pouring

To evaluate the quality of poured concrete, crosshole sonic logging (CSL) test was conducted to assess the integrity of the diaphragm wall [26]. Several tubes, typically with an inside diameter of 30 mm, were tied to the reinforcement cage before concrete pouring. These tubes were filled with water after concrete pouring. A pair of ultrasonic probes of identical resonant frequencies were dropped onto the bottom of two tubes, and then retracted to the top while continuously generating and receiving sound waves through the concrete. During the period of retracting, the wave speed, amplitude, distortion and attenuation of the received waveform were monitored in detail. The integrity of A2-b59, A2-a57, as well as the joints between them was tested. The speed and amplitude of waves along the depth of the secondary panel A2-b59 are shown in Fig. 11. The wave speed and amplitude were both larger than the corresponding critical values along the whole depth in all three monitored sections, indicating high integrity of the diaphragm wall. Data monitored for A2-a57 and the joint between A2-a57 and A2-a59 showed the same trend, and thus were omitted for conciseness.

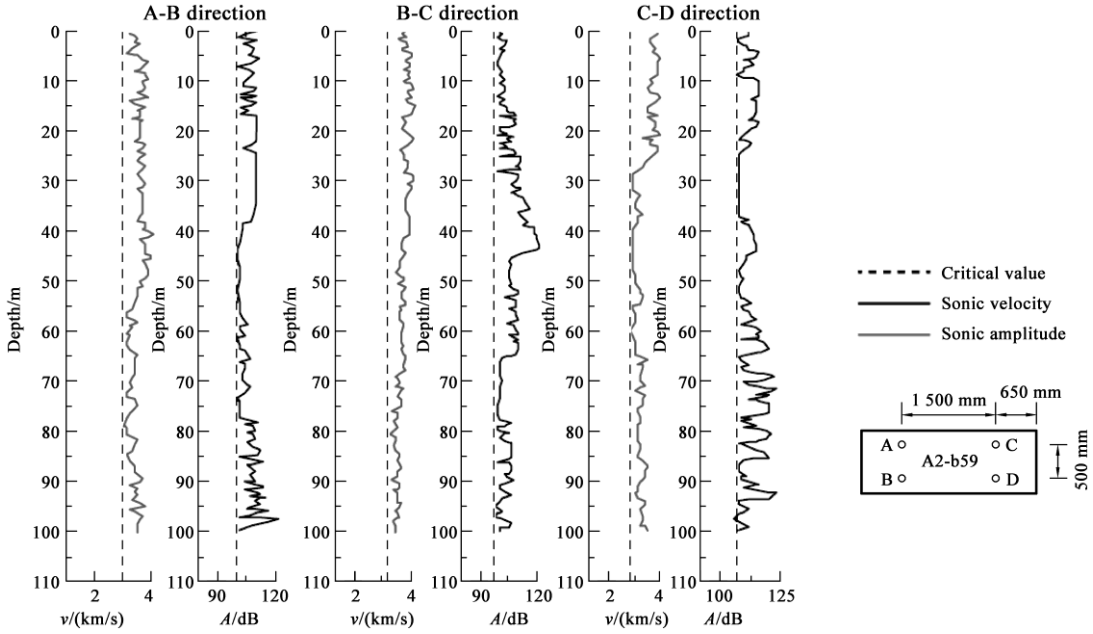

Fig. 11 Test result of the CSL (A2-b59), where *v* is the sonic velocity and *A* is the sonic amplitude

4 Instrumentation and monitoring program

Fig. 12 illustrates the layout of the in-situ test and monitoring instrumentation. The monitoring instruments consisted of settlement markers, inclinometers, and magnetic rings. Settlement markers spanned over the 2.8 m part of panel A2-a57 close to the middle panel, and they were arranged in three columns at a horizontal spacing of 1.4 m. The transverse distance between the first row of settlement markers and the diaphragm wall was 2 m, the transverse distance between the first and second rows was 3 m, and that between the second and third rows was 5 m. Each settlement marker system contains a steel rod, the bottom of which must be at least 0.5 m below the ground surface. Three boreholes B-1, B-2, B-3 were drilled at distances of 1 m, 5 m and 10 m away from the A2-b59 panel, respectively. The depth of three boreholes was limited to be 50 m to avoid crossing the confined aquifer. This is sensible as the deformation of the upper soil mass is of greater essence. The inclinometer system and magnetic ring system were installed within the three boreholes to monitor the lateral and vertical soil displacement along the depth during the process of construction. The magnetic ring system, which was used to measure the vertical displacement, consisted of 12 magnetic rings distributed at a vertical spacing of 4 m within the excavation depth ranging from −4 m to −48 m.

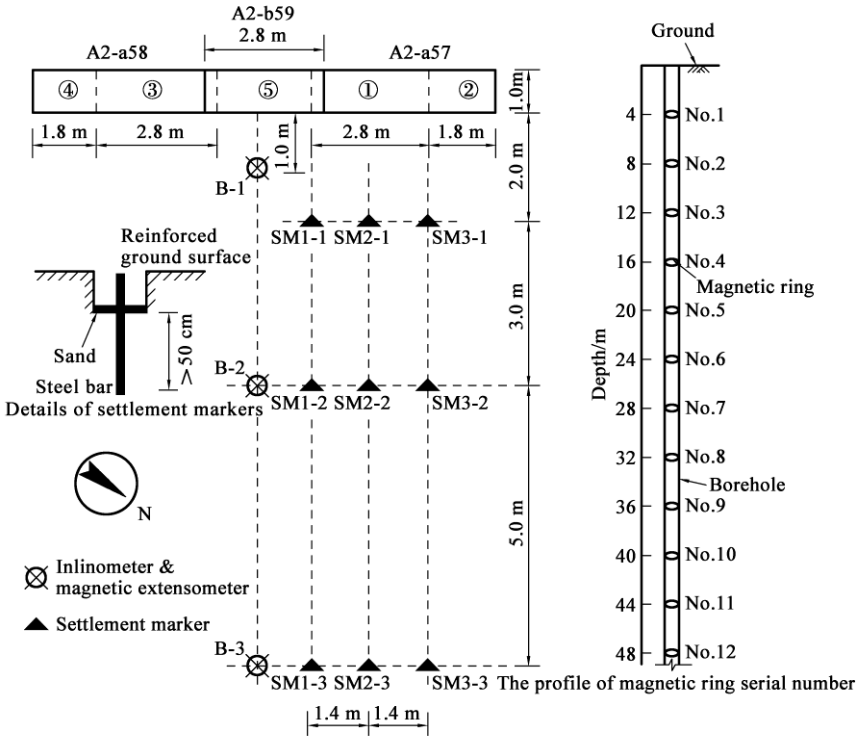

Fig. 12 Layout of the field testing program and monitoring instrumentation

5 Monitoring results and discussion

5.1 Ground surface settlement

Fig. 13 presents the ground settlement at different transverse distances with respect to the diaphragm wall versus the depth of trenching. The mean values of the three measuring points were adopted to represent the corresponding settlement at different depths. A turning point is identified at the trenching depth of 30 m for all three curves, after which the slope of settlement curves becomes steeper. Referring to Fig. 2, this turning point corresponds to the interface between the clayey layer and sandy layer. The increased slope in the sandy region may result from seepage and deterioration of slurry. Fig. 13 also shows that the maximum ground settlement reached 12.5 mm, which is approximately 0.11% of D (here D denotes the trenching depth of the diaphragm wall). The ground settlement decreased as the transverse distance of the measurement points to the diaphragm wall increased. The influence zone of excavation was limited to regions with a transverse distance smaller than 5 m from the diaphragm wall.

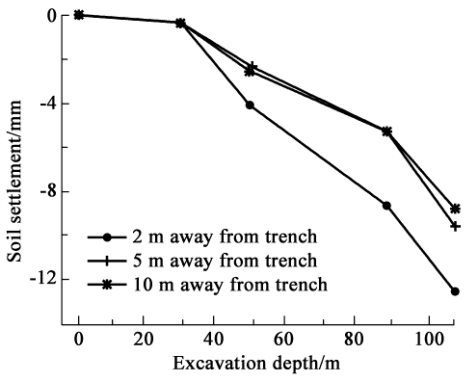

Fig. 13 Comparison of the soil surface settlement along trenching depth at different locations

5.2 Lateral displacement

Fig. 14 shows the lateral displacement curves of B-1, B-2 and B-3 boreholes during the construction of the secondary trenching panel A2-b59. The lateral displacement towards the trench was taken as positive. Four characteristic trenching stages were considered, including trenching at depths of 30 m, 50 m, 110 m and completion of concrete casting.

The lateral displacements at B-1 and B-2 increased initially as excavation depth increased until a primary peak value was reached, below which the lateral displacements decreased and eventually became more or less constant; whereas no obvious lateral displacement appeared at B-3. This indicates that the influence area of trench excavation did not extend beyond 10 m horizontally away from the trench. The primary peak may mark the location of a global failure, which was likely to happen as the muddy clay had a sensitivity of up to 4.4. The excavation depth at which the primary peak lateral displacement occurred was located in the clayey stratum, and decreased as the transverse distance of the borehole to the trench increased. The lateral displacement increased as trenching proceeded, but it recovered a bit due to the increase of lateral pressure induced by concrete pouring. However, the effect of concrete pouring was not significant as the coefficient of concrete filling was very close to 1 (see Table 4). The lateral displacement curves are quite smooth in the clayey soil strata; in contrast the lateral displacement curves fluctuate in the sandy soil strata, which may be induced by local collapse of trench walls.

To investigate the lateral displacement characteristics of different soil strata along the transverse direction, the mean values of measured lateral displacements over a certain range of buried depth were calculated to explicitly represent the overall lateral deformation of a specific stratum. This simplification enabled us to consider the distinct behavior of different soil strata subject to unloading of in-situ stresses. Fig. 15 shows the distribution of overall lateral deformations with varying distance to

the trench for three different strata (i.e., muddy clay, silt clay, and sandy silt) at the trenching depth of 110 m. The mean lateral displacements of all three strata decreased with increasing distance to the trench and dropped to almost 0 mm at the distance of 10 m. The lateral displacement of muddy clay was the largest.

5.3 Vertical displacement

Fig. 16 shows the vertical displacement obtained from the three boreholes spaced perpendicular to the secondary panel A2-b59. Fig. 16a illustrates the vertical displacement profiles of three boreholes at the end of trenching. The vertical displacement of B-1 which was the borehole nearest to the trench, was the most pronounced. Two peak points corresponding to vertical displacements of 18 mm and 33 mm were identified at depths −12 m (clayey layer) and −40 m (sandy silt layer), respectively. The vertical displacement profile of B-2 was similar to that of B-1, while the vertical displacement of B-3 was not obvious compared with that of B-1 and B-2.

Table 4 Summary of concrete pouring volumes

Panel	Theoretical volume/m^3	Actual volume/m^3	Coefficient of concrete filling
A2-a57	478	480	1.01
A2-a58	470	482	1.02
A2-b59	305	320	1.05

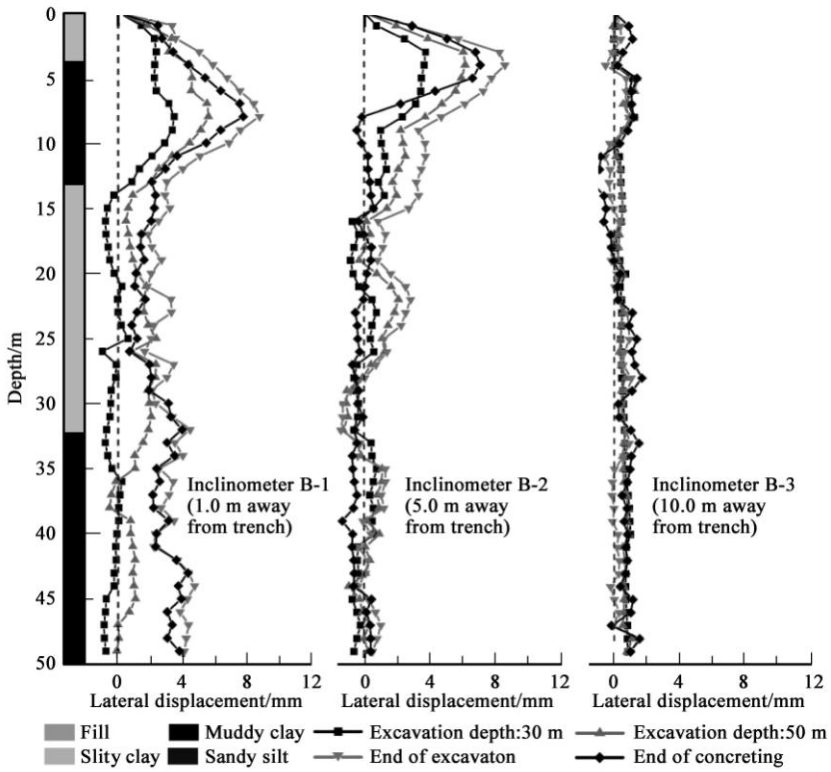

Fig. 14 Lateral ground deformation at different stages of diaphragm wall construction, where a positive value refers to a displacement toward the trench

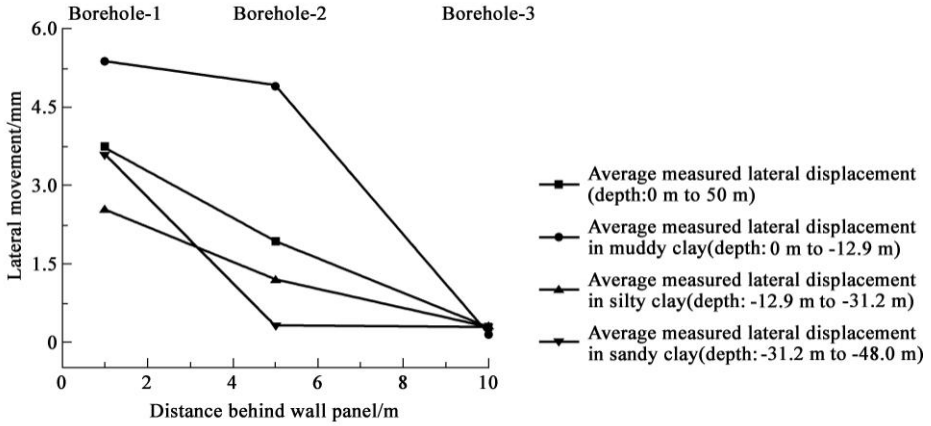

Fig. 15 Average lateral soil movement of different strata at various distances to the test wall panel

Fig. 16b shows the evolution of the vertical displacement profile at different stages of construction. Overall, the vertical displacement increased continuously as trenching proceeded. The increment of the vertical displacement was quite obvious between the end of trenching and the onset of concreting, especially in sandy silt. The monitored vertical displacements at the depths of −40 m and −48 m were increased by 80% and 83% from the end of trenching to the onset of concreting.

The soil in clayey layer (corresponding to the depth of 0 to −36 m) rebounded subject to concrete pouring due to the increasing concrete pressure. However, the monitoring data from the magnetic rings No.10 to No. 12 (corresponding to the depth of −40 m to −48 m) show that the vertical displacement still increased in the sandy silt layer. This might be caused by local collapse of trench wall due to deterioration of slurry induced by of falling of fine soil particles.

Fig. 17 presents the variation of vertical displacement in different construction stages at selected depths in three strata: muddy clay, silty clay and sandy silt. The tendency of the curves can be categorized into two different patterns. In both muddy clay and silt clay, the vertical displacement tended to increase during the period of trenching and then decreased during the period of concreting. The vertical displacement within the silty clay layer became stable at the end of concreting, while it still evolved at the end of concreting in the muddy clay layer due to its plastic flow state and high sensitivity to construction disturbance. The development of vertical displacement in the sandy silt did not cease even after concreting. In particular, there was a sudden drop between the end of trenching and the onset of concreting. This was because the sandy silt had low cohesion and contained a high proportion of fine particles smaller than 0.05 mm. These fine particles were likely to fall into the slurry, which thereby reduced the slurry quality. Figs. 16 and 17 indicate that slurry circulation and desanding should be performed more frequently when trenching in sandy silt layers.

6 Conclusion

This paper presents a case history of an ultra-deep diaphragm wall project in China, which served as a pilot project for the construction of a deeply-buried water storage tunnel beneath the Suzhou River in Shanghai. The trenching technologies, quality control measures and the ground responses due to construction disturbance were examined. The main observations and experience gained from this pilot project are listed below.

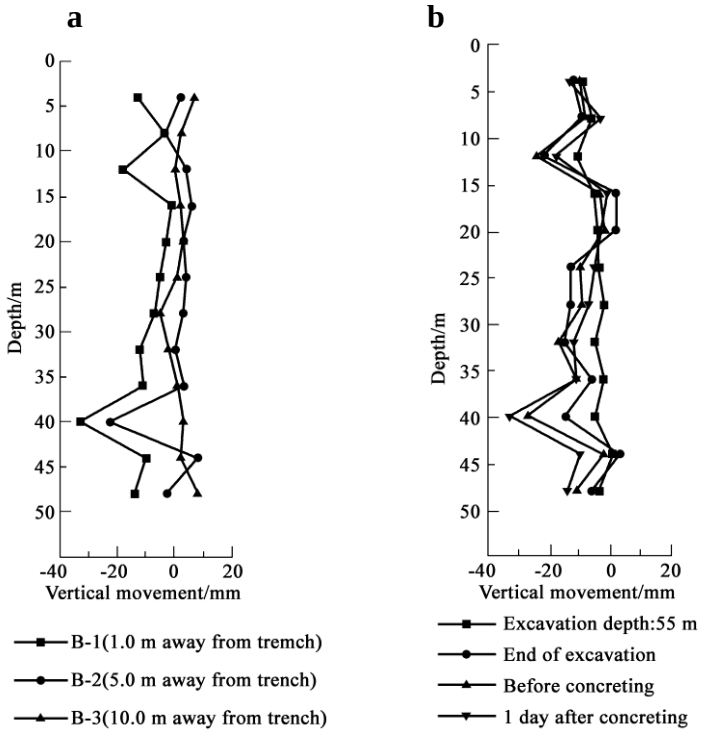

Fig. 16 Soil vertical displacement profiles: a) 3 boreholes 1day after concreting; (b) different periods of B-1

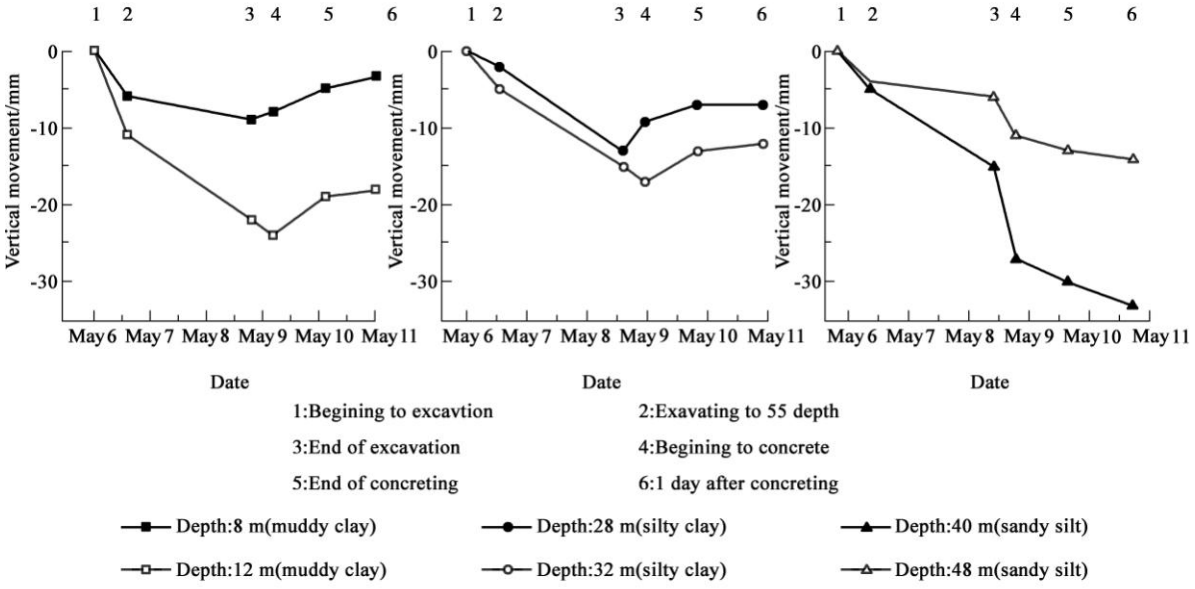

Fig. 17 Comparison of the soil displacement within different strata at different construction stages

In view of construction techniques:

1) The overcutting method using a Bauer BC40 cutter machine in conjunction with cutter wheels specified to different strata has been proved to be

qualified to construct diaphragm walls as deep as 110 m in soft soil areas. The construction efficiency and precision can be guaranteed given that the qualities of slurry and poured concrete are well controlled.

2) Using a reasonable casting velocity and at the mean time maintaining a smooth rise of concrete level could effectively reduce the risk of localized collapse of trench face and thereby ensure the integrity of the wall.

Mechanically, different strata behaved differently subject to trenching:

3) The surface settlement developed more rapidly when trenching in sandy silt layers than that in clayey layers, which may be attributed to seepage and deterioration of slurry. The influence zone of trench excavation did not extend beyond the area 10 m transverse from the diaphragm wall, which was within 10% of the total excavation depth.

4) The lateral displacement profile along the excavation depth appeared smooth in the muddy clay layer with a local peak, while the lateral displacement profile in sandy silt layer oscillated. This indicates that a global sliding failure may have happened in the muddy clay layer at a certain depth beneath the ground surface, whereas local instability failure may have taken place in the sandy silt layers.

5) Careful attentions should be paid to the sandy silt layer throughout the construction as the vertical displacement of the sandy silt continued to evolve even after concrete pouring.

The aforementioned knowledge and experience will be of great value to future construction of the ultra-deep diaphragm walls in soft soil areas of China.

Acknowledgements

The research was conducted with funds provided by the National Basic Research Program of China (973 Program, No.2014CB046905), the National Natural Science Foundation of China (Grant Nos. 41172249 and 51509186) and the State Key Laboratory for Geomechanics and Deep Underground Engineering (No. SKLGDUEK1303). The fund provided by Zhuhai Da Heng Qin Company Limited (Grant No. SG25-2014-173B1) is also appreciated.

References

[1] KOO D H, JUNG J K, LEE W. Sustainability applications for storm drainage systems minimizing adverse impacts of global climate change [C]// Proceedings of the International Conference on Pipelines and Trenchless Technology 2012: Better Pipeline Infrastructure for a Better Life. Reston, Virginia: American Society of Civil Engineers, 2013: 36-47.

[2] SARASWAT C, KUMAR P, MISHRA B K. Assessment of stormwater runoff management practices and governance under climate change and urbanization: an analysis of Bangkok, Hanoi and Tokyo [J]. Environmental Science & Policy, 2016, 64: 101-117.

[3] TAKAHASHI H. Underground drainage river system project promoted by the Tokyo metropolitan government [C]// International Workshop on Floodplain Risk Management. Hiroshima: [s.n.], 1996: 289-299.

[4] MARTINEZ-AUSTRIA P, BANDALA E R. Issues and challenges for water supply, storm water drainage and wastewater treatment in the Mexico City metropolitan area [M]. London: Routeledge, 2015: 109-125.

[5] KUESEL T R, KING E H, BICKEL J O. Tunnel engineering handbook[M]. New York: Van Nostrand Reinhold Co, 1982.

[6] NORDMARK A. Overview on survey of water installations underground: underground water-conveyance and storage facilities [J]. Tunneling and Underground Space Technology, 2002, 17(2): 163-178.

[7] COWLAND J W, THORLEY C B B. Ground and

building settlement associated with adjacent slurry trench excavation [C]// Proceedings of the Third Conference on Ground Movements and Structures. Cardiff: Forecasting, 1984: 723-728.

[8] LIU C, ZHANG Z, REGUEIRO R A. Pile and pile group response to tunneling using a large diameter slurry shield-Case study in Shanghai [J]. Computers and Geotechnics, 2014, 59(59): 21-43.

[9] FARMER I W, ATTEWELL P B. Ground movements caused by a bentonite-supported excavation in London clay [J]. Géotechnique, 1972, 23(4): 576-581.

[10] POH T Y, WONG I H. Effects of construction of diaphragm wall panels on adjacent ground: field trial [J]. Journal of Geotechnical and Geoenvironmental Engineering, 1998, 124(8): 749-756.

[11] RIGBY D B, LEI G H, NG S W L. Observed performance of a short diaphragm wall panel [J]. Géotechnique, 1999, 49(5): 681-694.

[12] Tsai J S, Jou L D, Hsieh H S. A full-scale stability experiment on a diaphragm wall trench [J]. Canadian Geotechnical Journal, 2000, 37(2): 379-392.

[13] OU C Y, YANG L L. Observed performance of diaphragm wall construction [J]. Geotechnical Engineering Journal of the SEAGS & AGSSEA, 2011, 42(3): 41-49.

[14] ELSON W K. An experimental investigation of the stability of slurry trenches [J]. Géotechnique, 1968, 18(1): 37-49.

[15] VOL N. Ground response during diaphragm wall installation in clay: centrifuge model tests [J]. Géotechnique, 1996, 46(4): 725-739.

[16] ZHUO H C, YANG Y Y, ZHANG Z X, et al. Stability of long trench in soft soils by bentonite-water slurry [J]. Journal of Central South University, 2014, 21(9): 3674-3681.

[17] MORGENSTERN N, AMIR-TAHMASSEB I The stability of a slurry trench in cohesionless soils [J]. Géotechnique, 1965, 15(4): 387-395.

[18] TSAI J S, CHANG J C. Three-dimensional stability analysis for slurry-filled trench wall in cohesionless soil [J]. Canadian Geotechnical Journal, 1996, 33(5): 798-808.

[19] NG C W W, YAN R W M. Three-dimensional modelling of a diaphragm wall construction sequence [J]. Géotechnique, 1999, 49(6): 825-834.

[20] BRUNNER W G. Development of slurry wall technique and slurry wall construction equipment [C]// GeoSupport 2004: Proceedings of the Innovation and Cooperation in the Geo-Industry. Florida: [s.n.], 2004: 520-529.

[21] CHEN J J, WANG J H, QIAO P, et al. Shear bearing of cross-plate joints between diaphragm wall panels–I: model tests and shear behavior [J]. Magazine of Concrete Research, 2016, 68(17): 902-915.

[22] 宋刚.连续墙铣槽机铣轮优化设计试验研究[D].北京:中国地质大学,2012.
SONG G. Design optimization for diaphragm trrench cutting wheel [D]. Beijing: China University of Geosciences, 2011. (In Chinese).

[23] SPAGNOLI G, BI A, WEIXLER L. Trench cutter case histories and their possible application for offshore piles as relieve drilling [J]. Geotechnical and Geological Engineering, 2014, 32(3): 713-724.

[24] PAUL D. Slurry walls: design, construction, and quality control [M]. Philadelphia: American Society for Testing and Materials Special Technical Publication, 1992.

[25] BRUCE D A, DEPAOLI B, MASCARDI C, et al. Monitoring and quality control of a 100 meter deep diaphragm wall [C]// Proceedings of the International Conference on Piling and Deep Foundations. London: [s.n.], 1989: 15-18.

[26] MENDEZ J A, RAUSCHE F, ASCE M. Quality control of diaphragm walls by crosshole sonic logging [C]// Proceedings of the GeoCongress 2012. Oakland: Geocongress, 2012: 650-663.